Original Article

Repairing of rabbit calvarial defects by rapid prototyping BisGMA and hydroxy-appatite incorporated BisGMA

Naris Thengchaisri[1*] Chaiyakorn Thitiyanaporn[1] Siriporn Tanodekaew[2]

Abstract

The in vivo bone regenerative capacity and biocompatibility of bisphenol A glycidylmethacrylate (BisGMA) implants fabricated by Stereolithography Rapid Prototyping machine (SLA) was investigated in rabbit's calvarial defect model. The study focused on two different materials: BisGMA alone and hydroxyapatite (HA) incorporated BisGMA, of which were formulated especially for SLA fabrication. Each rabbit's skull implant was fabricated with size 1x1 cm^2 according to the rabbit skull's contour based on its Computed Tomographic data and replaced at the full thickness cavarial defects in 6 rabbits. Computed Tomography (CT) scan and blood tests were performed at certain time points during 6 months after surgical operation to evaluate the bone regenerative capacity and biocompatibility. CT images revealed that the newly formed bone was gradually increased according to the implantation periods and all rabbit skulls showed good healing response without adverse tissue reactions. There was no remarkable difference in bone regeneration compared between BisGMA and HA incorporated BisGMA. After 24 weeks, the implants with surrounding skull tissues were removed and observed for cellular response of bone to implants. Scanning electron microscope revealed more callus formation surrounding the BisGMA (3.87±0.05 mm) compared to HA incorporated BisGMA (3.21±0.22 mm, $P = 0.023$). From histological studies, BisGMA implants were encapsulated with thicker fibrous tissue compared to HA incorporated BisGMA, suggesting that HA incorporated BisGMA induced less tissue reaction. Based on the present study in a rabbit calvarial defect model, it is concluded that SLA provides a well fitting implant. Furthermore, incorporation of HA to BisGMA improves biological compatibility with less fibrous tissue encapsulation.

Keywords: bone, composite, hydroxyapatite, rabbit, skull

[1]*Department of Companion Animal Clinical Sciences, Kasetsart University, Bangkhen, Bangkok 10900 Thailand*
[2]*National Metal and Materials Technology Center 114 Thailand Science Park, Klong Luang, Pathumthani 12120 Thailand*
****Correspondence**: ajnaris@yahoo.com* (N. Thengchaisri)
Received February 28, 2020.
Accepted August 18, 2020.

Introduction

Cranioplasty, the repair of a skull vault defect by insertion of implant materials, is widely used for anatomical reconstruction, brain protection and cosmetics. The indications of cranioplasty are decompressive craniectomies (DC), skull tumor or congenital defect (Dujovny *et al*., 1997; Greene *et al*., 2008). Recently, materials for skull reconstruction are bone allograft/autograft, the synthetic bone substitute materials, or polymethymethacrylate (PMMA)(Caro-Osorio *et al*., 2013). PMMA, a transparent thermoplastic, is first used during the World war II in 1940s for cranioplasty (Elkins and Cameron, 1946). Nowadays, PMMA is commonly used as bone replacement which is frequently required to substitute damaged tissue from any trauma or disease occurring in cranioplasty. The infection rate of PMMA implant case was not significantly different when compared with autogenous bone flap (Klinger *et al*., 2014). This PMMA implant is normally prepared in the operation room with free-hand forming, thus it is difficult to make it perfectly fit to the patient's bony defect contour and also takes more operation time waiting for PMMA to set. Custom implants using 3D printing technologies such as stereolithography provide better cosmesis in craniofacial surgery. Moreover, PMMA is associated with poor osteointegration with minimal attachment effect to nearby bone tissue, thus, development of better biocompatible for craniofacial implant is needed.

In this study, bisphenol A glycidylmethacrylate (BisGMA) was formulated to be photosensitive especially for Stereolithography Rapid Prototyping machine (SLA) to fabricate the implants instead of PMMA. With the biocompatible properties of BisGMA, which is widely used as composites and sealants in dentistry (Pratap *et al*., 2019), combined with the outstanding freeform fabricating object of rapid prototyping machine, the rabbit's skull implants which is safe to use and perfect fit to the bone defect were fabricated. Furthermore, effects of incorporation of hydroxyapatite (HA) into the BisGMA materials for SLA fabrication might improve the biological properties, since HA is an essential element for development of bone tissue.

The aims of this study were to compare the biocompatibility and effect on bone regeneration of skull implants made from BisGMA alone and HA incorporated BisGMA which were fabricated by SLA.

Materials and Methods

Animals: This study was approved by the Kasetsart University Institutional Animal Care and Use Committee (ACKU02253) and by the Ethical Review Board of the Office of National Research Council of Thailand (NRCT license No. U1-07457-2561). Six adult, skeletally mature, male/female New Zealand white rabbits were used in this study. All rabbits were older than three months and weighed between 2.6 and 2.8 kg. The skull defects were made on both sides of skull of each rabbit for implantation with BisGMA and BisGMA incorporated with HA, while the BisGMA alone was treated as a control group. All rabbits were sacrificed at the 24th week after the operation.

Material Fabrication: In this study, Bisphenol A glycidyl methacrylate (BisGMA; Esstech Inc., Essington PA, USA) was formulated for SLA by adding triethylene glycol dimethacrylate (TEGDMA; Esstech Inc., Essington PA, USA) as a reactive diluent at 30%-wt, then further mixed with camphorquinone (Esstech Inc., Essington PA, USA) and N,N dimethylaminoethyl methylacrylate (Fluka Chemical Corp, Switzerland) as a photoinitiator and a reducing agent (Dimethyl amino pyridine 4-EDMAB Ethyl-4-dimethyl amino benzoate, DMPT), respectively, was used as based resin. This formulated BisGMA was used either alone or in combination with hydroxyapatite (HA; Taihei Chemical Industrial Co. Ltd., Japan).

Fabrication of Skull Implant by Stereolithography Rapid Prototyping: Before conducting rabbit calvarial defect model, 3D digital model of BisGMA implant was designed by using Materialise Software, Mimics13.1 and Magic 9.5, according to each rabbit's skull contour based on 3D-CT scan data (Philips 64 Slice CT Scan). The 10.0 x 10.0 x 1.0 mm implants were fabricated layer-by-layer by the Stereolithography rapid prototyping machine which is equipped with a 200 mW visible laser source using laser wavelength at 473 nm (Jeong *et al*., 2009) with 75 µm in diameter of laser spot size. Two types of materials, BisGMA and BisGMA added with 5% HA (by weight), were used to fabricate the implants for close the rabbit's skull defects. After implants were fabricated, the materials were washed with isopropyl alcohol for several minutes, post-cured in a halogen-light box for 1 hr and sterilized by steam prior to implantation.

Surgical Procedure: All rabbits were anesthetized with an intra-muscular dose of ketamine (15 mg/kg) and xylazine (5 mg/kg). After proper preparation, the parietal bone was exposed through a skin incision approximately 3 cm in length over the linea media. Two separated square bone defects (size of 10.0 x10.0 mm) were created using a 1 mm round burr on a slow-speed electric hand piece by applying 0.9% physiologic saline irrigation. After the bone was removed, the carvarial defects in the right and the left sides were closed by BisGMA and HA incorporated BisGMA, respectively (Fig. 1). The closure of subcutaneous tissues was performed with 4/0 polyglyconate (Maxon; Johnson & Johnson (Thailand) Limited, Thailand) with a simple interrupted suture pattern and the skin was relocated with 3/0 Nylon (Ethilon; Johnson & Johnson (Thailand) Limited, Thailand) with a simple continuous suture pattern. Subcutaneous injection of enrofloxacin (Baytril; Bayer Thai Co., Ltd., Thailand) at 10 mg/kg was administered once daily on the day of surgery until 10 days after surgery. The animals were euthanized at 24 weeks after implantation, and the defects were dissected with an additional 5.0 mm surrounding tissue from the host bone. All the harvested samples were fixed in a 4% paraformaladhyde solution buffered by 0.1 M phosphate solution (pH 7.2) for 3–5 days before further analysis.

3D computed tomography (CT) analysis: Blood test and spiral 3D-CT scan (1024 x 1024 matrix) were

performed at 1, 6, 12 and 24 weeks post-operatively for evaluation the in vivo biocompatibility and bone regenerative capacity. Cessation of wound healing and bone formation in cranial defects should complete within twelve weeks (Hollinger and Kleinschmidt, 1990). In this study, 24 weeks was chosen as the endpoint for monitoring further on long term side effects. In every scan, all rabbits were tranquilized with an IM injection (10 mg/kg) of ketamine. The scan was taken by 64 Slice CT Scan (GE Philips, at voltage 120kV and electrical current of 120-150 mA) at a thickness of 0.5 mm. Based on the CT data (in DICOM file type), the 3D digital models of rabbit's skull were reconstructed, selected the ROI (region of interested), superimposed and the defect areas were compared by Materialise Software (the 3D digital models of rabbit's skull were reconstructed, selected the ROI (region of interested), superimposed and the defect areas were compared by Materialise Software (Mimics13.1 and Magic 9.5; Materialise, NV).

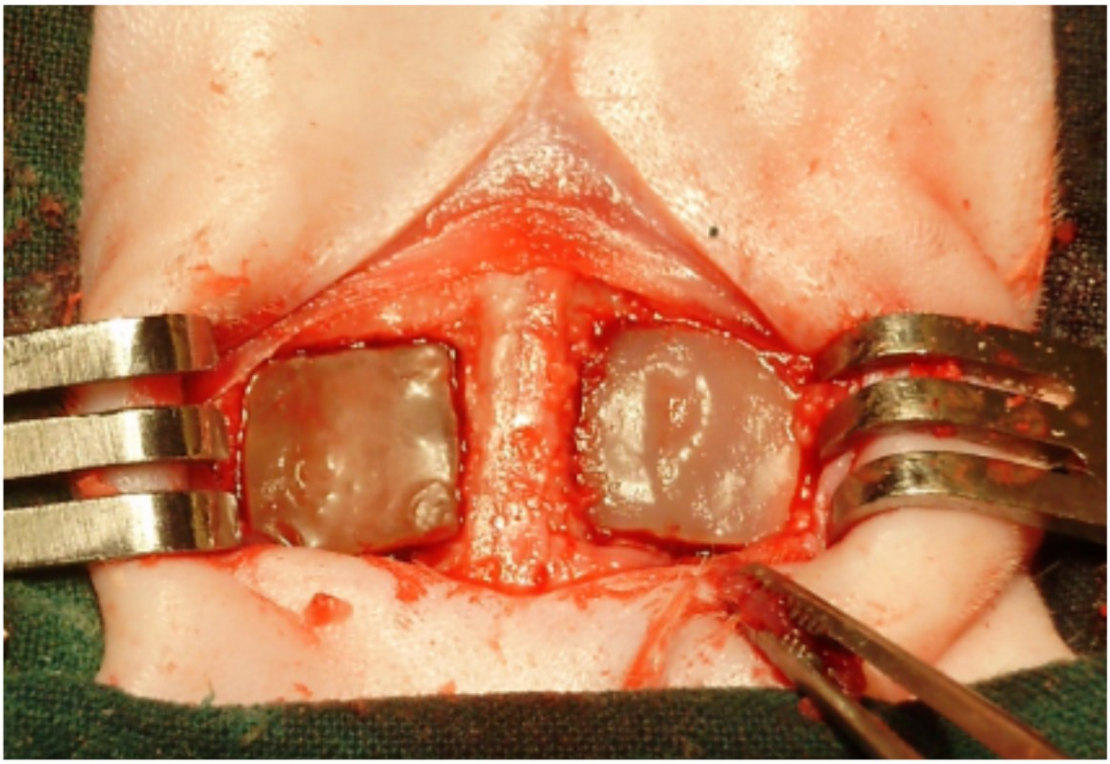

Figure 1 Intra-operative picture of rabbit skull defect model of the present study.

Scanning electron microscope (SEM) and Histological analysis: All rabbits were euthanized at 24th week post-operatively with an intravenous injection of pentobarbital (45 mg/kg). The cranial defects with surrounding skull tissues were harvested, immersed in a solution of 2% (v/v) glutaraldehyde in PB and prepared for SEM (n = 3) and histological investigation (n = 3). The skull's specimens were cross-sectioned using a precision cutting machine (Struers Model Accutom-5) equipped with a metal-bonded diamond cut-off wheel. The sectioned samples were dehydrated by graded ethanol changes and critical point dry, and subsequently gold sputtered in vacuum before examination by SEM (JSM-5410 LV; JOEL Ltd., Japan). The small pieces of sectioned samples (less than 2 mm^2) were decalcified with 14.28% (w/v) EDTA solution and processed for embedding in Spurr resin. After hardening, the blocks were cut to a thickness of 1-2 µm using LKB UltrotomeV, and stained with hematoxylin and eosin (H&E). Histological observations were carried out using an inverted light microscope (Olympus IX71) equipped with a digital camera (Olympus DP72; Olympus (Thailand) Co., Ltd., Thailand). The osteogenesis, wound healing and the condition of the surrounding soft tissue were compared between BisGMA and HA incorporated BisGMA. The new bone formation on top and bottom was calculated based on the surface area on the top and bottom of the implant. The value was expressed in percentage based on the surface area.

Statistical analysis: The statistical analysis in the present study was conducted using STATA12 (StataCorp, College Station, Texas, USA) and GraphPad Prism Version 6 (GraphPad Software, San Diego, California, USA). All data were tested for normality using a Shapiro-Wilk test. A paired t-test was used to compare the percentage of newly formed bone covering between two types of SLA implants. The significant level was set at $P < 0.05$.

Results

The 3D images of newly formed bone, which reconstructed from CT scan data, were observed after implantation at 1, 6, 12 and 24 weeks (Fig. 2). From these 3D images, the averaged percentage of newly formed bone at the different time after implantation of both implant materials were calculated (Fig. 3). The average percentage of newly formed bone of week 6^{th}, 12^{th} and 24^{th} of BisGMA alone is 40.84%, 63.52% and 83.17% and BisGMA in combination with HA is

48.23%, 71.15% and 84.36%, respectively. There was no significant different on bone formation between BisGMA and BisGMA in combination with HA at any time point ($P > 0.05$).

The skull was removed after 24 weeks of implantation. From SEM images of cross section, both implants (Fig. 4A) were surrounded by fibrous connective tissue but newly formed bone was observed extensively only at the bottom surface along the dura matter. The average callus thickness in BisGMA implants (3.87±0.05 mm) was significantly higher than HA incorporated BisGMA implants (3.21±0.22 mm) ($P = 0.023$, Fig. 4B).

The encapsulation of implants with fibrous tissue was also revealed from histological sections (Fig. 5). The BisGMA incorporated with HA implant was easily distinguishable by a well dispersing of HA particles in the resin matrix. Bone regeneration was observed in a similar pattern for both implants which found particularly dense of adipose tissue around the bottom of implants. The cell migrations were less contributed from the upper periosteum as a fairly number of adipose tissues was observed at the top part of implants. Newly formed bone was however not in close contact with the implant surface. There was no inflammatory reaction observed in both implants. It can also observe from light microscopy that the thickness of implant's surrounded fibrous tissue of BisGMA incorporated with HA implant is less than the BisGMA alone.

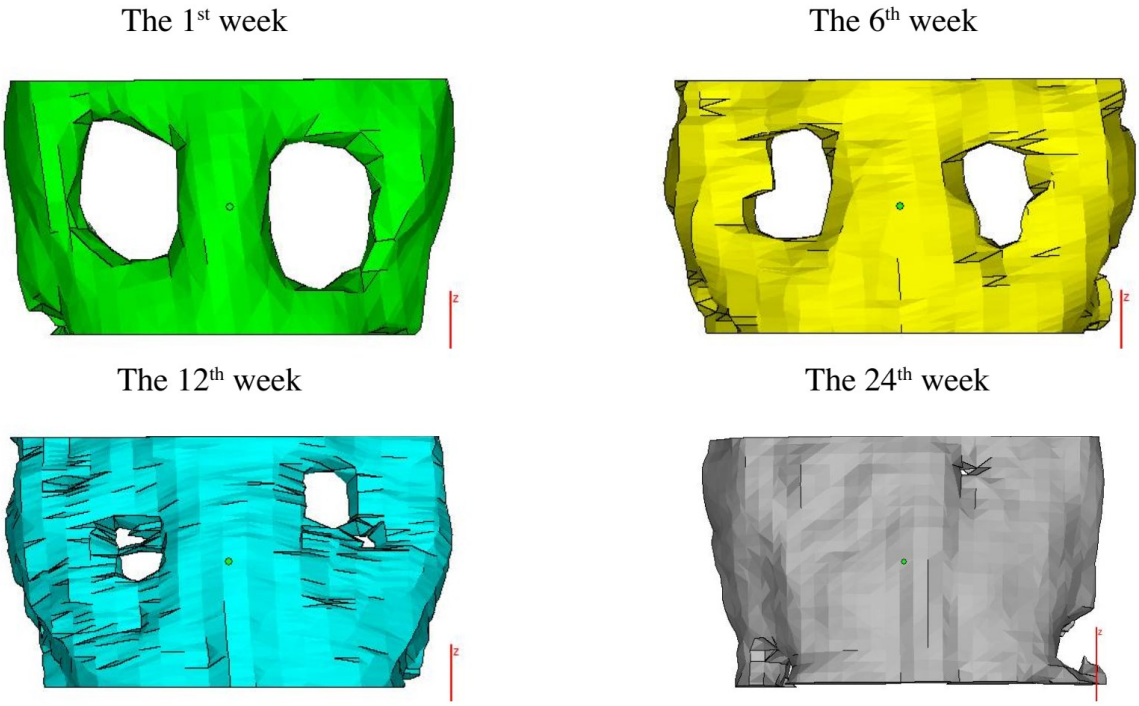

Figure 2 Three dimentional (3D) image reconstruction of newly formed bone after implantation for A: at 1 week after surgery, B: at 6 weeks after surgery, C: at 12 week after surgery, and D: at 24 weeks after surgery.

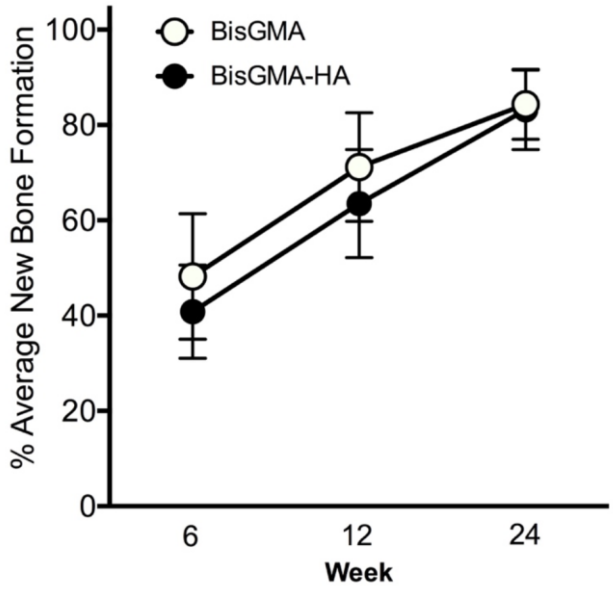

Figure 3 Percentage of newly formed bone covering the skull defects between BisGMA and BisGMA in combination with HA.

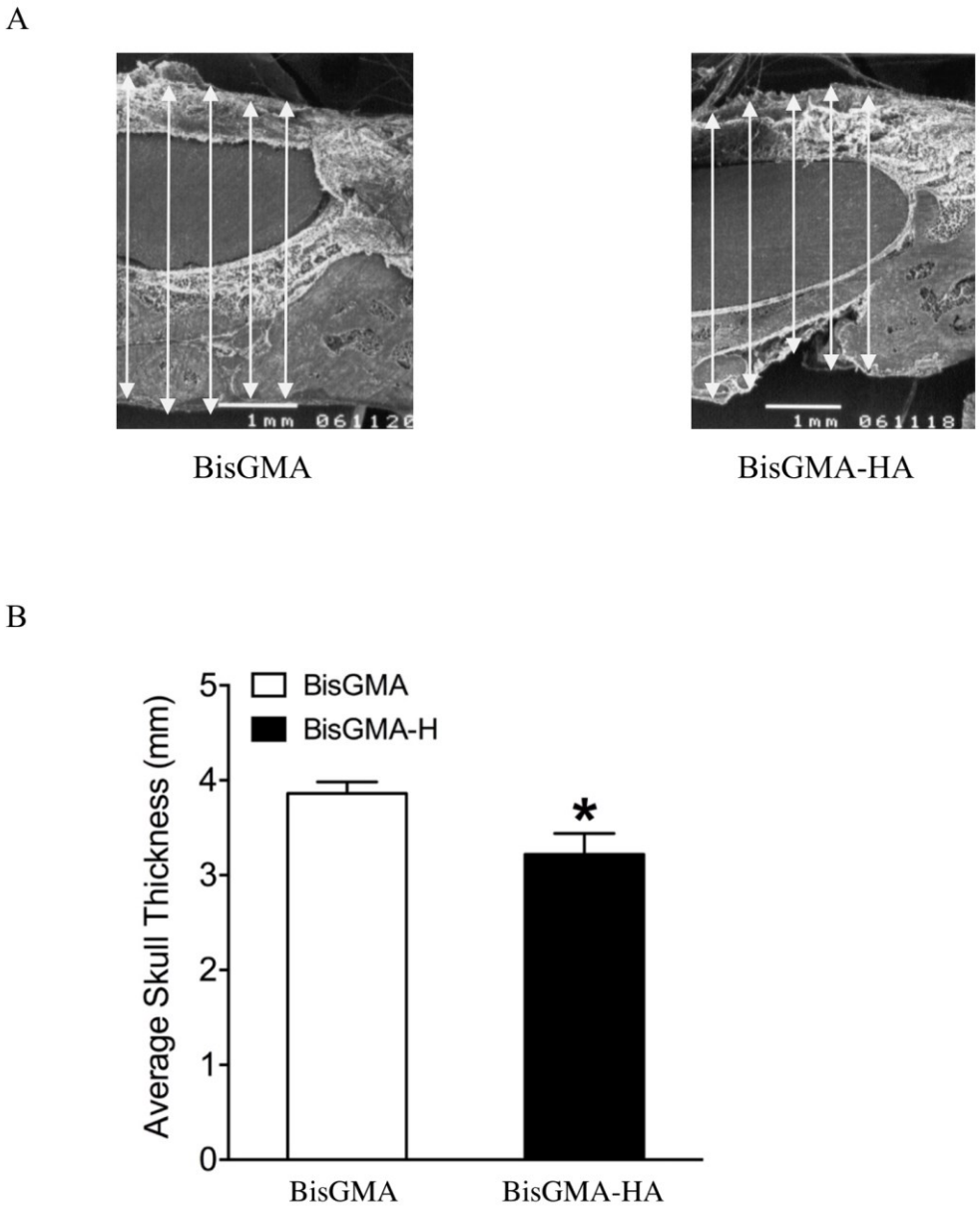

Figure 4 Scanning Electron Microscopic images of a cross-sectioned skull after 24 weeks implantation. A: Immage from scanning electron microscop comparing the BisGMA implant and the HA incorporated BisGMA implant on rabbit skull (n = 3). B: A bar graph compared skull thickness over BisGMA and HA incorporated BisGMA implants. *$P < 0.05$

Discussion

Many types of implants have been used in cranioplasty surgery. The ideal of cranioplasty material should meet criteria for biocompatibility, mechanical strength and inert in order to prevent inflammation, rejection or infection (Zaccaria *et al*., 2016). In addition, it has to possess optimal osteointegration and shows the good outcome of cosmetic result (Shah *et al*., 2014; Staffa *et al*., 2012; Staffa *et al*., 2007). The autologous bone graft is still the preferred choice in children's skull defect repair (Appelboom *et al*., 2011; El Ghoul *et al*., 2015; Frassanito *et al*., 2015). However, the synthetic materials that could be made on demand and specific purposes have become increasing used for skull defect repair surgery. These included titanium mesh, acrylic bone cement (PMMA), alumina ceramic, hydroxyapatite and pre-shaped polyetheretherketone implants (PEEK) (D'Urso *et al*., 2000; Eppley, 2005; Lee *et al*., 2009; Shah *et al*., 2014).

The most common problem in cranio-maxillo-facial surgery is the complexity of bony defect contouring which is difficult to shaping the bone substitute material to perfectly cover the defect. Normally the bone substitutes have to be shaped free-hand intra-operatively which prolongs both the operation time and further compromise the recovery of the high-risk patient. This risk can be reduced by shorten the operation time by preparation the implant prior surgery. SLA has been recently used for fabrication the implants with its excellence in complex shape fabrication (D'Urso *et al*., 2000). Another critical point that needs to be concerned is material's safety and biocompatibility. BisGMA which is certified on biocompatibility and widely used in dentistry (Pratap *et al*., 2019) was chosen as implant's material for SLA fabrication.

Incompatible implants may induce an extensive biological cascade of adverse cellular responses characterized by chronic inflammatory response surrounding the implants, bone degration and bone necrosis (Bitar and Parvizi, 2015). In the present study, we did not observe leukocytes infiltration on both implants at twenty-four week after surgery, suggesting both implants induce minimal tissue reaction. Moreover, all rabbits tolerated the surgical procedures well and there was no reduction in body weight and no post-operative infection in all rabbits. From 3D images of newly formed bone, it was clearly seen that the newly formed bone increased with the increasing of the implantation periods and also the bone regeneration rate was found better in HA incorporated BisGMA than the BisGMA alone. From the histological analysis it showed that all implants were surrounded by a fibrous layer. SEM and Light microscopy images illustrated that the surrounded fibrous was constructed of the new bone regeneration at the bottom of implants. There was no close contact between the implant surface and newly formed tissue and no inflammatory reactions was observed in both implants. These suggested that the osteogenic cells migrated mostly from the edge of bone defect or the underlying dura mater to form the new bone tissue. From light microscopy images it is clearly seen that the thickness of osteogenic cells at the junction between the edge of bone defect and BisGMA incorporated with HA implant is much less than the implant made by BisGMA alone which means that BisGMA incorporated with HA has better biocompatibility and less biological reactivity. The present study suggested the clinical usefulnesss of a 3D printing implants using BisGMA incorporated with HA for providing not only patient-specific implant but also better biocompatible to bone tissue than BisGMA material alone.

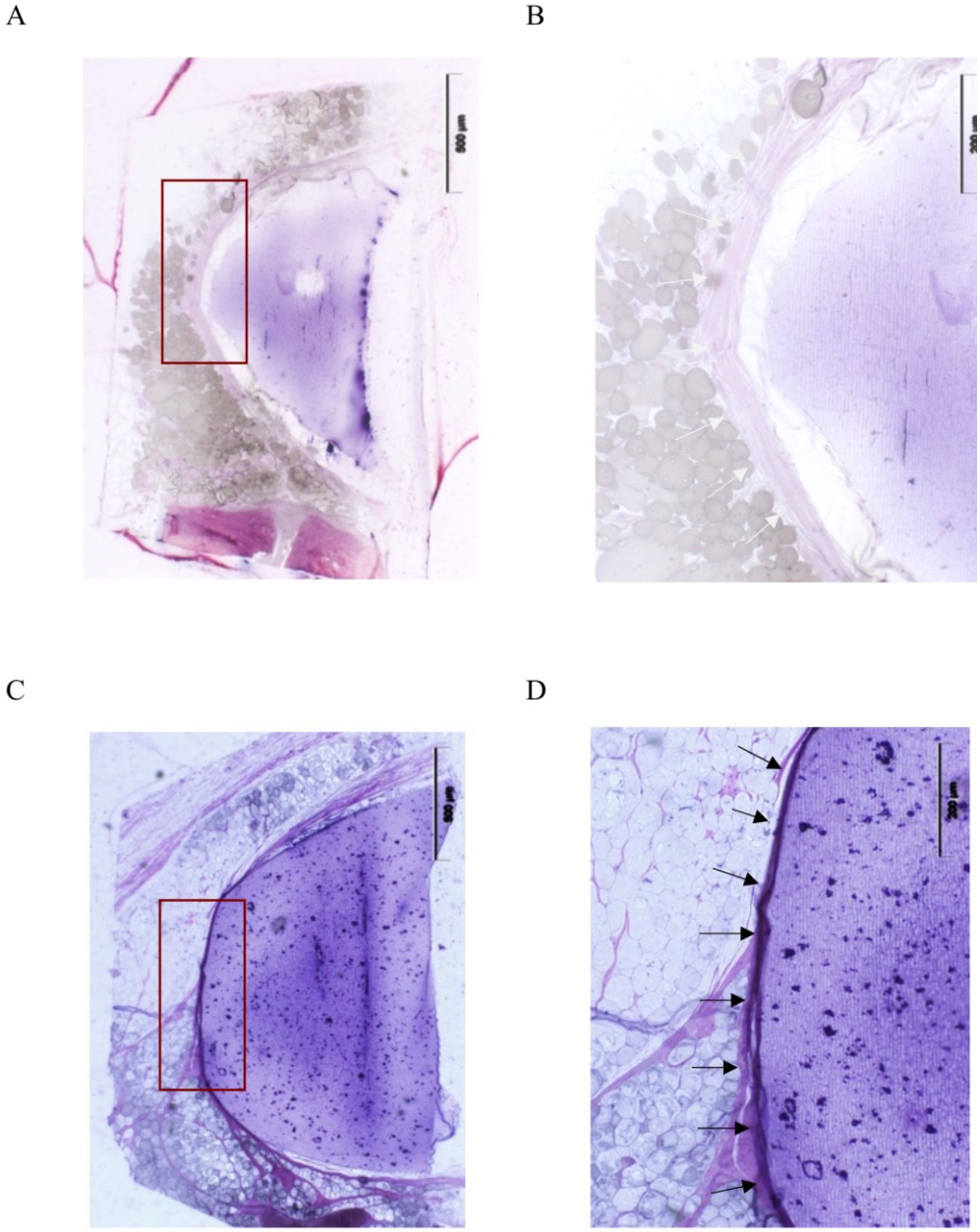

Figure 5 Histological examination of a cross-sectioned skull with H&E staining after 24-week calvarial implantation. A: BisGMA implant (10x magnification), B:BisGMA implant (20x magnification), C: HA incorporated BisGMA implant (10x magnification), D: HA incorporated BisGMA implant (20x magnification). Bar indicates 200 μm in length.

BisGMA was formulated to polymerize at wavelength 473 nm (Jeong *et al*., 2009). In the present study, the three-dimensional implants fabricated by SLA technique were made from BisGMA alone and HA incorporated BisGMA. Addition of 5% HA to the BisGMA did not affect the polymerization process, but improved bone regeneration capability of rabbit skulls with less fibrous tissue encapsulation. The shrinkage of BisGMA may occur between 5-12% depending on the type of diluents used, thus adjustment of 3D structure should be made before printing (Ligon *et al*., 2017). The weakness of the present study includes a lack of data to compare each time point for healing process and tissue reaction. However, the long-term effects of SLA implants were observed at 24 weeks using SEM and histological analysis. It should be noted that the design for SLA technique used in the present study was unabsorbable. Although the implant materials may provide a strong protective craniofacial implant but it may prevent bone healing process due to a lack of material porosity. Lacking porosity of the implant also prevented vascularization and new bone formation.

In conclusion, the result of this study demonstrated that BisGMA and HA incorporated BisGMA implants fabricated by SLA was nicely fit to the rabbit skull contour and compatible to the surrounding tissue. HA incorporated BisGMA improved the property of the BisGMA based materials by minimizing callus formation and less fibrous tissue encapsulation surrounding the materials compared to BisGMA alone.

Conflict of interest statement: None of the authors of this paper has a financial relationship with other people or organizations that could inappropriately influence or bias the content of the paper.

Acknowledgements

This study was partly supported by grants from KURDI and Faculty of Veterinary Medicine, Kasetsart University, to Dr.Thengchaisri. We'd like to thank Dr.Kriskrai Sitthiseripratip, Mr. Tratat Apatthananon, Ms. Paweena Uppanan, Ms. Somruethai Channasanon, for their technical supports.

References

Appelboom G, Zoller SD, Piazza MA, Szpalski C, Bruce SS, McDowell MM, Vaughan KA, Zacharia BE, Hickman Z, D'Ambrosio A, Feldstein NA, Anderson RC. 2011. Traumatic brain injury in pediatric patients: evidence for the effectiveness of decompressive surgery. Neurosurg Focus. 31(5): E5.

Bitar D, Parvizi J. 2015. Biological response to prosthetic debris. World J Orthop. 6(2): 172-189.

Caro-Osorio E, De la Garza-Ramos R, Martinez-Sanchez SR, Olazaran-Salinas F. 2013. Cranioplasty with polymethylmethacrylate prostheses fabricated by hand using original bone flaps: Technical note and surgical outcomes. Surg Neurol Int. 4: 136.

D'Urso PS, Earwaker WJ, Barker TM, Redmond MJ, Thompson RG, Effeney DJ, Tomlinson FH. 2000. Custom cranioplasty using stereolithography and acrylic. Br J Plast Surg. 53(3): 200-204.

Dujovny M, Aviles A, Agner C, Fernandez P, Charbel FT. 1997. Cranioplasty: cosmetic or therapeutic? Surg Neurol. 47(3): 238-241.

El Ghoul W, Harrisson S, Belli A. 2015. Autologous cranioplasty following decompressive craniectomy in the trauma setting. Br J Neurosurg. 29(1): 64-69.

Elkins CW, Cameron JE. 1946. Cranioplasty with acrylic plates. J Neurosurg. 3: 199-205.

Eppley BL. 2005. Biomechanical testing of alloplastic PMMA cranioplasty materials. J Craniofac Surg. 16(1): 140-143.

Frassanito P, Tamburrini G, Massimi L, Di Rocco C, Nataloni A, Fabbri G, Caldarelli M. 2015. Post-marketing surveillance of CustomBone Service implanted in children under 7 years old. Acta Neurochir (Wien). 157(1): 115-121.

Greene AK, Mulliken JB, Proctor MR, Rogers GF. 2008. Pediatric cranioplasty using particulate calvarial bone graft. Plast Reconstr Surg. 122(2): 563-571.

Hollinger JO, Kleinschmidt JC. 1990. The critical size defect as an experimental model to test bone repair materials. J Craniofac Surg. 1(1): 60-68.

Jeong TS, Kang HS, Kim SK, Kim S, Kim HI, Kwon YH. 2009. The effect of resin shades on microhardness, polymerization shrinkage, and color change of dental composite resins. Dent Mater J. 28(4): 438–45.

Klinger DR, Madden C, Beshay J, White J, Gambrell K, Rickert K. 2014. Autologous and acrylic cranioplasty: a review of 10 years and 258 cases. World Neurosurg. 82(3-4): e525-530.

Lee SC, Wu CT, Lee ST, Chen PJ. 2009. Cranioplasty using polymethyl methacrylate prostheses. J Clin Neurosci. 16(1): 56-63.

Ligon SC, Liska R, Stampfl J, Gurr M, Mulhaupt R. 2017. Polymers for 3D printing and customized additive manufacturing. Chem Rev. 117: 10212-10290.

Pratap B, Gupta RK, Bhardwaj B, Nag M. 2019. Resin based restor Resin based restorative dental materials: characteristics and future perspectives. Jpn Dent Sci Rev. 55(1): 126-138.

Shah AM, Jung H, Skirboll S. 2014 Materials used in cranioplasty: a history and analysis. Neurosurg Focus. 36(4): E19.

Staffa G, Barbanera A, Faiola A, Fricia M, Limoni P, Mottaran R, Zanotti B, Stefini R. 2012. Custom made bioceramic implants in complex and large cranial reconstruction: a two-year follow-up. J Craniomaxillofac Surg. 40(3): e65-70.

Staffa G, Nataloni A, Compagnone C, Servadei F. 2007. Custom made cranioplasty prostheses in porous hydroxy-apatite using 3D design techniques: 7 years experience in 25 patients. Acta Neurochir (Wien). 149(2): 161-170.

Zaccaria L, Tharakan SJ, Altermatt S. 2016. Hydroxyapatite ceramic implants for cranioplasty in children: a single-center experience. Childs Nerv Syst. 33(2): 343-348.